JOURNAL OF CATALYSIS **169,** 176–187 (1997)
ARTICLE NO. CA971675

A Study of the Feasibility of Incorporation of Chromium into the Molecular Sieve Framework: The Transformation of 1-Butene over Cr-Silicoaluminophosphate Molecular Sieves

D. Escalante, L. Giraldo, M. Pinto, C. Pfaff, V. Sazo, M. Matjushin, B. Méndez, C. M. López, F. J. Machado, J. Goldwasser,[1] and M. M. Ramírez de Agudelo*

*Centro de Catálisis, Petróleo y Petroquímica, Escuela de Química, Facultad de Ciencias, Universidad Central de Venezuela, Apartado Postal 47102, Los Chaguaramos, Caracas 1020-A, Venezuela; and *INTEVEP, S. A, Apartado Postal 76343, Caracas 1070-A, Venezuela*

Received November 18, 1996; revised February 21, 1997; accepted February 24, 1997

The catalytic transformations of 1-butene were performed over a chromium-substituted silicoaluminophosphate molecular sieve (CrAPSO-11), over a Cr-supported SAPO-11 molecular sieve (Cr/SAPO-11), and over two SAPO-11 samples. For times-on-stream under 2.5 h, the CrAPSO-11 catalyst showed a higher skeletal isomerization efficiency (SIE) than the two prepared SAPO-11 samples and the supported chromium system. After 2.5 h a drastic decrease in the SIE occurred (for the CrAPSO-11 sample) with a concomitant increase in the formation of butadiene and 2-butenes. The formation of butadiene was considerably hindered over the supported system compared to that of the CrAPSO-11 sample. The cracking reactions as well as the formation of C5+ hydrocarbons were also suppressed over the supported system. The catalysts were recently characterized by XPS and redox cycles (12) and presently studied by XRD, DRS, and NO chemisorption followed by IR spectroscopy and acidity measurements performed with pyridine chemisorption. A larger amount of Cr(VI) was found by DRS and XPS (~70%) for the oxidic CrAPSO-11 (O_2, 773 K), compared to the supported system. For the latter, Cr(III) was the main species present. The NO chemisorption experiments showed the presence of high chromium oxidation states on the oxidic CrAPSO-11. After reduction (H_2, 773 K), the distribution of oxidation states of chromium (XPS and NO chemisorption experiments) for the reduced CrAPSO-11 solid, was different ~40% Cr(VI) and ~60% Cr(III) compared to the oxidic sample. Cr(VI) showed a higher stability towards reduction in the CrAPSO-11 catalyst when compared to chromium supported on conventional supports. The distribution of oxidation states of chromium was very similar for the oxidic and the reduced Cr/SAPO-11 catalyst. The oxidic CrAPSO-11 catalyst showed an increase in the number of medium + strong acid sites compared to the other catalysts. The reduction process, however, decreased the Brønsted strong acid sites by a factor of two. A concomitant decrease was observed for the medium + strong Lewis acid sites, upon reduction. These results suggest that a partially unsaturated Cr(VI) in the vecinity of P–OH groups may act as strong Lewis sites, generating Brønsted acidity by Brønsted–Lewis interaction, as suggested in the literature. The supported sample showed a decrease of medium + strong Brønsted acid sites compared to the CrAPSO-11 solid. In this case, however, the reduction process did not cause major changes in the acidity distribution. The characterization as well as the catalytic data support and reinforce the model presented by Chen and Sheldon (*J. Catal.* 153, 1 (1995)) for the related CrAPO-5 system. The results suggest the incorporation of chromium into the molecular sieve framework for the CrAPSO-11 catalyst.

INTRODUCTION

The skeletal isomerization of *n*-butenes has been thoroughly studied on a variety of catalytic systems for over 30 years (1–7). Several reaction mechanisms as well as different reaction intermediates have been proposed to account for the formation of isobutene (1–7). Recently, this reaction has regained a great deal of attention due to the strategic importance of isobutene in the manufacture of methyl tert-butyl ether (MTBE), a valuable octane booster oxigenated fuel additive (7, 8).

Silicoaluminophosphates (SAPOs) and metal-substituted silicoaluminophosphates (MeAPSOs) are among the catalytic systems reported active (9–11) for the transformations of 1-butene. Particularly, the CrAPSO-11 system was shown to be very selective toward isobutene during the first 2.5 hours-on-stream, dropping suddenly to less than 7% after 200 min (10). Reduction by the hydrocarbon of Cr(VI) and Cr(V) to Cr(IV), leading to an increase in Brønsted acidity, was suggested to explain the increase in selectivity for isobutene during the early stages of the reaction. Further reduction to Cr(III), with a concomitant reduction in Brønsted acidity, was invoked to explain the drop in selectivity observed for times-on-stream (TOS) larger than 2.5 h.

Recently, we performed a study of the oxidation states of chromium for a CrAPSO-11 molecular sieve and for a supported Cr/SAPO-11 sample (12). The techniques

[1] To whom correspondence should be addressed. Dr. José Goldwasser, E-mail: jgoldwas@strix.ciens.ucv.ve.

0021-9517/97 $25.00

employed were X-ray photoelectron spectroscopy (XPS) and reduction-oxidation (H_2–O_2) cycles. XPS results showed that only two chromium 2p doublets (Cr(VI) and Cr(III)) were necessary to curve fit the experimental data. For the oxidic samples, a higher percentage of Cr(III) species was found in the supported sample. The difference between both samples remained following reduction (H_2, 773 K). For the CrAPSO-11 sample, Cr(VI) showed a higher stability toward reduction, compared to chromium supported on conventional supports. These data suggested incorporation of Cr(VI) into the silicoaluminophosphate framework for the CrAPSO-11 catalyst, as suggested by Chen and Sheldon (13a) for the CrAPO-5 system.

The possible incorporation of chromium into the silicoaluminophosphate structure, besides its important academic implications, may render solids potentially selective for other desirable transformations such as dehydrogenation (13b), dehydroisomerization and oxidation reactions (13a).

In view of the above discussion, it was considered important to perform the transformations of 1-butene over both catalytic systems (CrAPSO-11 and supported Cr/SAPO-11) and compare the results with those obtained over two samples of SAPO-11 catalysts. Other techniques such as diffuse reflectance spectroscopy (DRS), NO chemisorption and acidity measurements (on the oxidic and reduced samples) were used as characterization tools. The results will be used in conjunction with the previous XPS and redox cycles data (12) to ascertain the feasibility of incorporation of chromium into the molecular sieve framework. The latter is the main objective of the present work.

EXPERIMENTAL

I. Catalysts

The synthesis procedure for the SAPO-11 preparations was reported elsewhere (14). Two SAPO-11 samples will be used throughout this work. SAPO-11-A corresponds to sample S-2 (Table 1 of Ref. 14) while SAPO-11-B corresponds to sample S-7 (Table 1 of Ref. 14). The preparation procedure used will be outlined here for the sake of completion. The source of alumina (pseudoboehmite, Catapal B from Vista Chemical Co.) was added to a diluted phosphoric acid (Aldrich) solution and stirred for 1 or 2 h. The organic template, di-n-propylamine (DPA) (Aldrich) was then added, and the mixture was again stirred for 1 or 2 h. Finally, the source of silica (40% SiO_2 colloidal silica, Ludox AS40 from Dupont) was incorporated, at room temperature, under vigorous stirring (1 or 2 h) until a homogeneous gel was obtained. For SAPO-11-A, the stirring time for each step was 2 h while for the SAPO-11-B a stirring time of 1 h, for each step, was used. The gel molar composition for both preparations was $Al_2O_3 : P_2O_5 : 0.3SiO_2 : DPA : 50H_2O$. The gels were transferred into 60-ml, Teflon-lined stainless-steel autoclaves and heated at 473 K for 24 h. The solid product recovered by centrifugation was thoroughly washed with distilled water and dried at 383 K overnight. To remove the amine the solid was calcined at 773 K for 15 h. The molar composition formula TO_2 was $Al_{0.48}P_{0.47}Si_{0.05}O_2$ for the SAPO-11-A and $Al_{0.544}P_{0.386}Si_{0.071}O_2$ for the SAPO-11-B.

The synthesis of the CrAPSO-11 was performed according to Flanigen *et al.* (19). The preparation procedure was as follows: the alumina source was added to the diluted solution of phosphoric acid and the mixture was stirred for 1 h. Thereafter, the source of silicon was added and the mixture stirred again for 1 h. The chromium promoter (chromium(III) hydroxiacetate (Aldrich)) was then incorporated, followed by a stirring period of 1 h. The addition of the amine, followed by a stirring period of 1 h, was the final step. All the reactants used in the synthesis of the SAPO's were used to synthezise the CrAPSO-11 solid. The gel molar composition was $0.9Al_2O_3 : P_2O_5 : 0.06Cr_2O_3 : DPA : 50H_2O : 0.3SiO_2$. A final crystallization temperature of 423 K and a crystallization time of 48 h were employed. The solid was first washed with distilled water and dried at 383 K for 16 h. The catalyst was then calcined under dry air at 813 K for 15 h in order to remove organic residues. The calcined solid had a molar composition (formula TO_2) $(Al_{0.39}P_{0.46}Cr_{0.033}Si_{0.11})O_2$. The Cr wt.% was 2.5. A supported Cr/SAPO-11 catalyst was prepared by impregnating a sample of SAPO-11-B with the same chromium promoter using the incipient wetness technique (3.6 wt.% Cr). The TO_2 formula for this solid was $(Al_{0.45}P_{0.41}Cr_{0.046}Si_{0.095})O_2$. For further experimental details see Ref. 14.

II. Procedures

X-ray diffractograms were recorded with a Philips diffractometer PW 1730 using Co-Kα radiation ($\lambda =$ 1.790255 Å) operated at 30 KV, 20 mA and scanning speed of 2° (2θ/min). For more details see Ref. 14.

Infrared spectra were recorded at room temperature using a Perkin-Elmer 1760X FTIR spectrometer with a resolution of 2 cm^{-1}. The IR cell described previously (15) had a built in furnace which was used to pretreat samples *in situ* at high temperatures. The cell could be attached to a conventional BET vacuum system (16, 17a). Samples were mounted in the cell as wafers having a thickness of approximately 15–20 mg/cm^2. Before the addition of NO or pyridine, the samples were treated overnight with O_2 (60 cm^3/min) at 773 K. The catalyst was evacuated ($P \leq 2.10^{-5}$ Torr) for 3 h at the same temperature and cooled to the corresponding chemisorption temperature under vacuum. After the oxidation pretreatment, some samples were cooled to room temperature and then exposed to pure H_2 (60 cm^3/min), with a subsequent increase

in the temperature (4 K/min) up to 773 K. The reduced catalyst was then evacuated for 1 h at 773 K and cooled to the chemisorption temperature under vacuum.

The NO chemisorption experiments were performed as follows: after the corresponding pretreatment, increasing doses of purified NO were admitted into the IR cell until the final pressure reached 50 Torr. The IR spectrum was registered after each dose of NO. The sample was then evacuated ($P \leq 2.10^{-5}$ Torr) for 1 h and the spectrum registered again.

The pyridine chemisorption experiments were carried out by exposing the pretreated sample to 5 Torr of pyridine vapor for 1 h at 363 K. The wafer was then evacuated for 1 h at different temperatures before the spectra were recorded. The outgassing temperatures used in the present work were 443, 623, and 723 K. The rationale to use these temperatures is to arbitrarily define the following acidity regions: strong (sites retaining pyridine at 723 K), medium + strong (sites retaining pyridine at 623 K), and total (weak + medium + strong) (sites retaining pyridine at 443 K). The normalized integrated intensities of the bands near 1547 cm^{-1} and 1450 cm^{-1} were used to calculate the amount of Brønsted and Lewis bound pyridine (Brønsted and Lewis acid sites), respectively, using the extinction coefficients given in Ref. 17b.

Diffuse reflectance spectra were recorded with a UV-VIS Perkin-Elmer spectrometer, scanning from 200 to 800 nm at a rate of 100 nm/min and a chart speed of 50 nm/cm. Alumina was used as a white reference.

Catalytic experiments were carried out in a conventional continuous flow system (10, 11) operated at atmospheric pressure. Preliminary experiments were performed to determine the reaction conditions for maximum steady-state formation of isobutene at a temperature where the dehydrogenation reaction would not be thermodynamically restricted. The reaction parameters used were: reaction temperature = 743 K, N_2 flow = 60 cm^3/min, 1-butene flow = 15 cm^3/min, weight of catalyst = 1 g. The reaction products were analyzed by on-line gas chromatography, using a Hewlett-Packard 5890 chromatograph with a flame ionization detector. A fused silica KCl/Al_2O_3 column was used for separation purposes. The catalytic tests were performed, for the calcined catalysts, after the solids were pretreated *in situ*, (N_2, 60 cc(STP)/min) overnight.

III. Data Treatment

For a reaction product (or set of products), the selectivity is defined by Eq. [1]

$$S_i = \left\{ A_i \Big/ \left(\sum A_i \right) - A_{1\text{-butene}} \right\} \times 100, \qquad [1]$$

where A_i is the corrected chromatographic area for a particular compound. The following selectivities were determined: S_{iso} (skeletal isomerization), $S_{2\text{-}b}$ (double bond isomerization), S_{diene} (formation of butadiene), S_{crack} (formation of C1–C3 products), S_{C5+} (formation of hydrocarbons with 5 or more carbon atoms). S_{crack} and S_{C5+} were calculated by including the sum of the corresponding hydrocarbons in the numerator of Eq. [1].

The total conversion (X) was calculated according to Eq. [2]:

$$X = \left\{ \left(\sum A_i \right) - A_{1\text{-butene}} \Big/ \sum A_i \right\} \times 100 \qquad [2]$$

The skeletal isomerization efficiency (SIE) is defined by Eq. [3]:

$$SIE = \{A_{isobutene}/(A_{isobut.} + A_{cis\text{-}2\text{-}but.} + A_{trans\text{-}2\text{-}but.}) \times 0.467\} \times 100 \qquad [3]$$

The 0.467 term corresponds to the isobutene equilibrium fraction at 743 K.

The skeletal isomerization specific activity (SISA) is defined by Eq. [4]:

$$SISA = (4.96 \cdot 10^{-5} \times WHSV \times X \times S_{iso})/AS, \qquad [4]$$

where WHSV = 2.06 h^{-1} (2.06 g of 1-butene/g of catalyst/h) and AS is the number of (medium + strong) Brønsted acid sites per g_{cat}, for the oxidic materials, calculated from the pyridine chemisorption experiments. The units for SISA are molecules of isobutene formed per second per acid site.

IV. Reagents

1-Butene was Matheson C. P. grade. Pyridine (Aldrich, spectrophotometric grade) was degassed using the freeze-pump-thaw technique (18). Nitric oxide (99.9%, Matheson) was purified by vacuum distillation between dry ice and liquid nitrogen traps (15). The oxygen and nitrogen (GIV) were passed over activated molecular sieve traps to remove traces of water. Hydrogen (GIV) was purified by being passed through a molecular sieve and commercial deoxo traps to remove water and oxygen traces. For further details on the reactants used in the synthesis procedure, see Ref. 14.

RESULTS

Figure 1 shows the XRD diffractogram for the calcined CrAPSO-11 sample. This diffractogram along with that obtained for the as- synthesized sample (12), show that the solid is highly crystalline with $AlPO_4$-11 (AEL) structure, in agreement with the literature (14, 19). The XRD results for the Cr/SAPO-11 system were similar to those reported for the SAPO-11-B support (14). No bulk phases corresponding to chromium oxides were detected in either case.

The DRS spectra for the calcined samples of both chromium preparations are shown in Figs. 2A and 2B (note differences in scales). For the CrAPSO-11 catalyst, two strong bands at 352 and 262 nm were detected. These

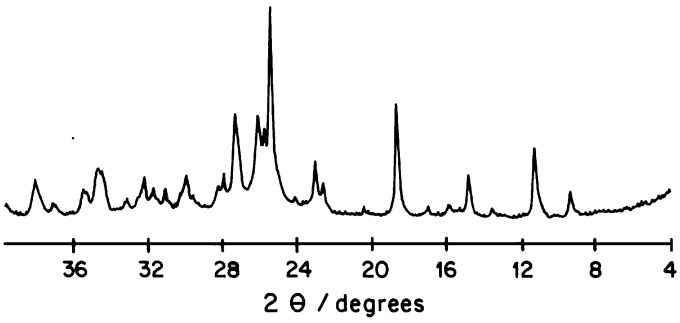

FIG. 1. XRD diffractogram for the calcined CrAPSO-11 sample.

bands have been assigned to charge transfer transitions $O \rightarrow Cr(VI)$ (20). A weak band around 447 nm was also observed. For the supported Cr/SAPO-11 sample, four bands at 453, 609, 365, and 271 nm were observed. The first two bands have been assigned to $^4A_{2g} \rightarrow {}^4T_{1g}$ and to $^4A_{2g} \rightarrow {}^3T_{2g}$ transitions, respectively, in Cr(III) systems (20, 21).

The IR spectra for the experiments involving NO are shown in Figs. 3–7. In all cases before addition of NO, the solids showed two small bands at ca. 1660 and 1840 cm^{-1}. Figure 3 shows the spectra for the stepwise addition of NO to the CrAPSO-11 catalyst evacuated at 773 K for 1 h, after the standard oxidation pretreatment. A sharp band at ca. 1627 cm^{-1} appears after the addition of small amounts of NO. Subsequent doses (up to 50 Torr) of NO generate two

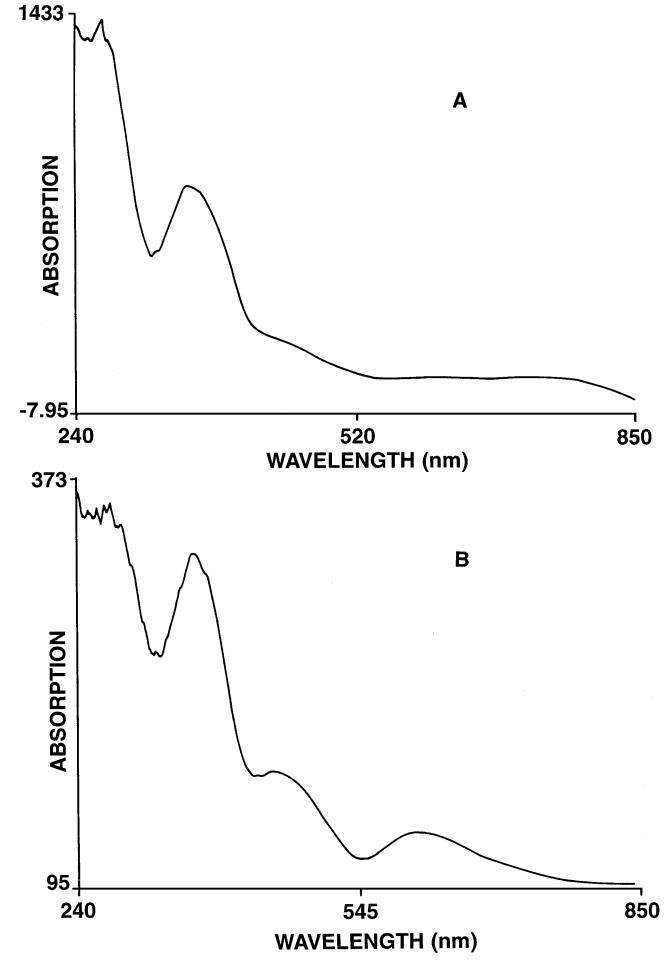

FIG. 2. Diffuse reflectance spectra for (A) the oxidic CrAPSO-11 and for (B) the oxidic Cr/SAPO-11 sample.

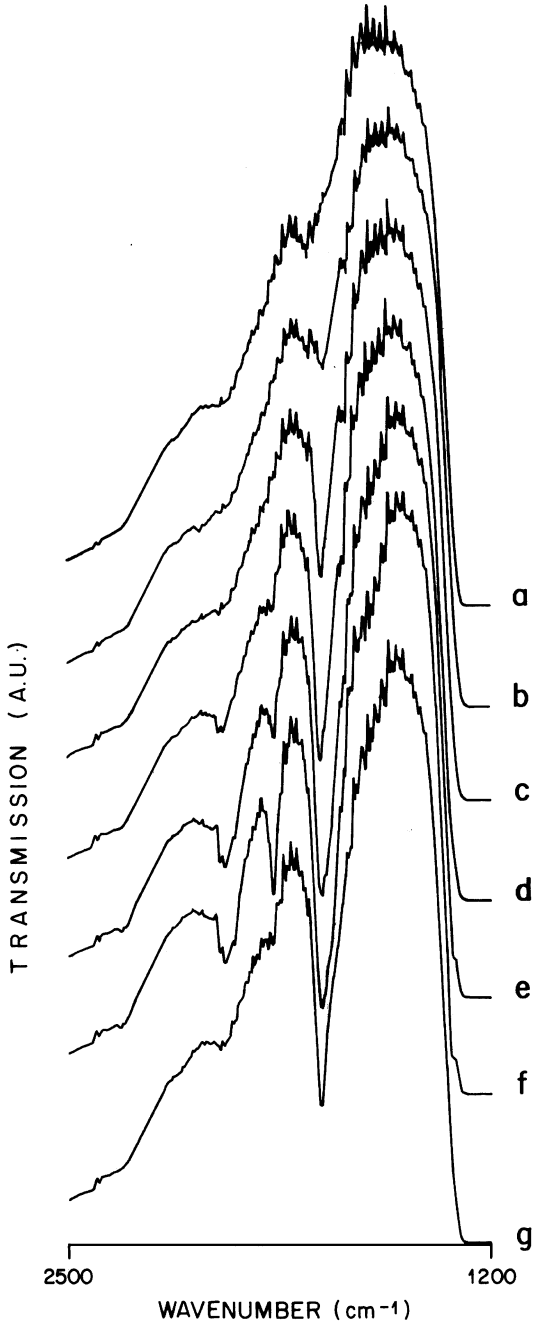

FIG. 3. Infrared spectra of nitric oxide adsorbed on the oxidic CrAPSO-11 catalyst evacuated at 773 K (a) before adsorption of NO, (b) after adsorption of 2 Torr of NO, (c) after adsorption of 5 Torr of NO, (d) after adsorption of 15 Torr of NO, (e) after adsorption of 50 Torr of NO, (f) after adsorption of 50 Torr of NO for 90 min, and (g) after evacuation at room temperature for 60 min following procedure (f).

new bands at ca. 1745 and 1860 cm^{-1}. These bands practically disappear after evacuation of the catalyst for 1 h at room temperature. To have a better understanding of the assignments for the mentioned bands, the following experiment was performed: after the CrAPSO-11 catalyst was given the standard oxidation pretreatment, the sample was cooled down under oxygen (room temperature) and then evacuated for 1 h. The spectra for the stepwise addition of NO are shown in Fig. 4. The same bands as for the catalyst evacuated at 773K, are observed. The intensity, however, is greatly increased for the 1627 and, particularly, for the 1745 cm^{-1} bands. The small high frequency band remains basically unchanged.

Figure 5 shows the IR spectra for CrAPSO-11 catalyst reduced at 773 K (H_2). Again, the same bands appear. In this case, however, the intensity is severely decreased, particularly for the 1745 cm^{-1}, which appears as a shoulder only after 50 Torr of NO have been added to the IR cell.

The 1900–1670 cm^{-1} spectral region is characteristic of mono- and dinitrosyls species adsorbed on supported Cr(III) and Cr(II) ions (22–24). Due to the similarity in frequencies, it is tempting to assign the 1745 and 1860 cm^{-1} bands to the asymmetric and symmetric stretching modes, respectively, of a dinitrosyl species. The results, however, show that the changes in intensity in one band are not accompanied by parallel changes in the other. Thus, apparently the two bands are not due to a common species. Another possibility, is that these two bands are generated by weakly held mononitrosyls species. In this case, two questions arise: why the observed increase in the intensity of the 1750 cm^{-1} band for the oxidic CrAPSO-11 evacuated at room temperature? Why the strong decrease in intensity observed for this band over the reduced catalyst? Seemingly, the bands at 1627 and 1750 cm^{-1} are favored over oxygen-rich chromium catalysts. The literature reports similar bands for NO_2 (25–27) and N_2O_4 (26, 28, 29) species respectively. Moreover, it has been shown for CrO_x/ZrO_2 catalysts, that NO reduces high Cr oxidation states to Cr(III), particularly on the freshly oxidized material (24). These two bands can, therefore, be taken as a diagnostic tool for the presence of high oxidation states of chromium, *vide infra*. The small 1860 cm^{-1} band can, in principle, be assigned to a weakly held form of a mononitrosyl complex.

A blank experiment was carried out on the oxidized SAPO-11 solids. The results are shown in Fig. 6 (SAPO-11-B). The original bands (before addition of NO) remain practically unchanged throughout the stepwise addition of NO to the solid. For the oxidic and reduced Cr/SAPO-11, the situation is very similar to that of the pure support. No new bands were observed upon the addition of NO. The results for the oxidic Cr/SAPO-11 are shown in Fig. 7.

Figures 8A and 8B show the IR spectra for the pyridine adsorption over the oxidic CrAPSO-11 and Cr/SAPO-11 catalysts, respectively, evacuated at 723 K. Only these spectra are shown due to the similar nature of the other IR data. The spectra were obtained by substracting the contribution from the sample before the adsorption of pyridine. The two

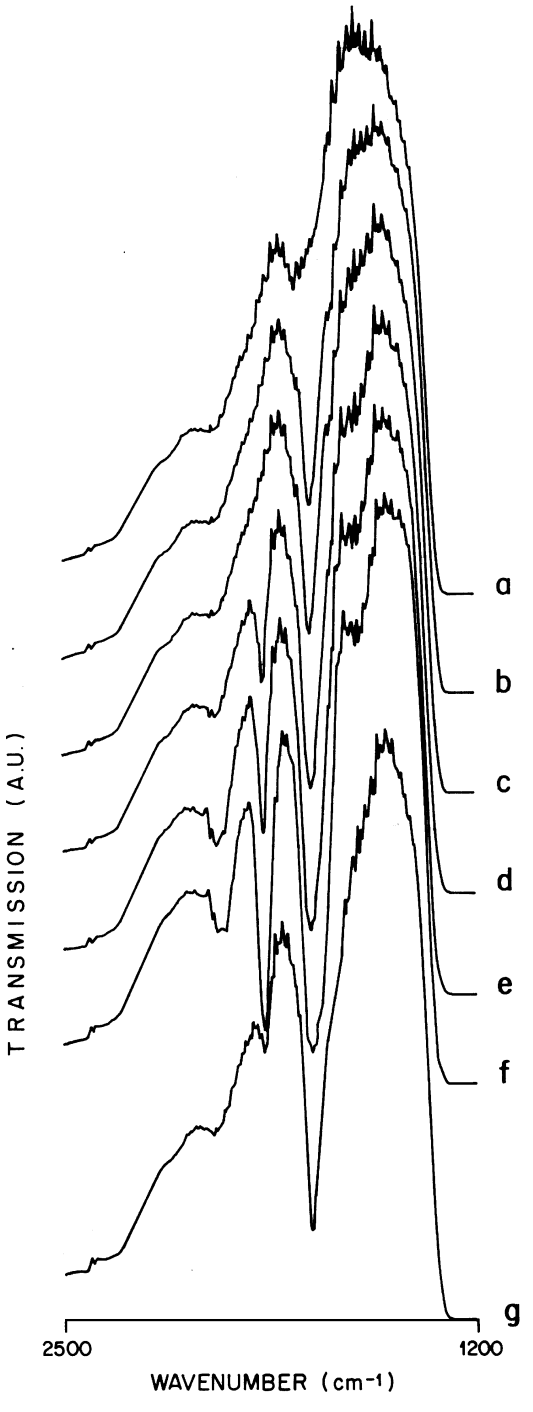

FIG. 4. Infrared spectra of nitric oxide adsorbed on the oxidic CrAPSO-11 catalyst evacuated at room temperature (a) before adsorption of NO, (b) after adsorption of 2 Torr of NO, (c) after adsorption of 5 Torr of NO, (d) after adsorption of 15 Torr of NO, (e) after adsorption of 50 Torr of NO, (f) after adsorption of 50 Torr of NO for 90 min, and (g) after evacuation at room temperature for 60 min following procedure (f).

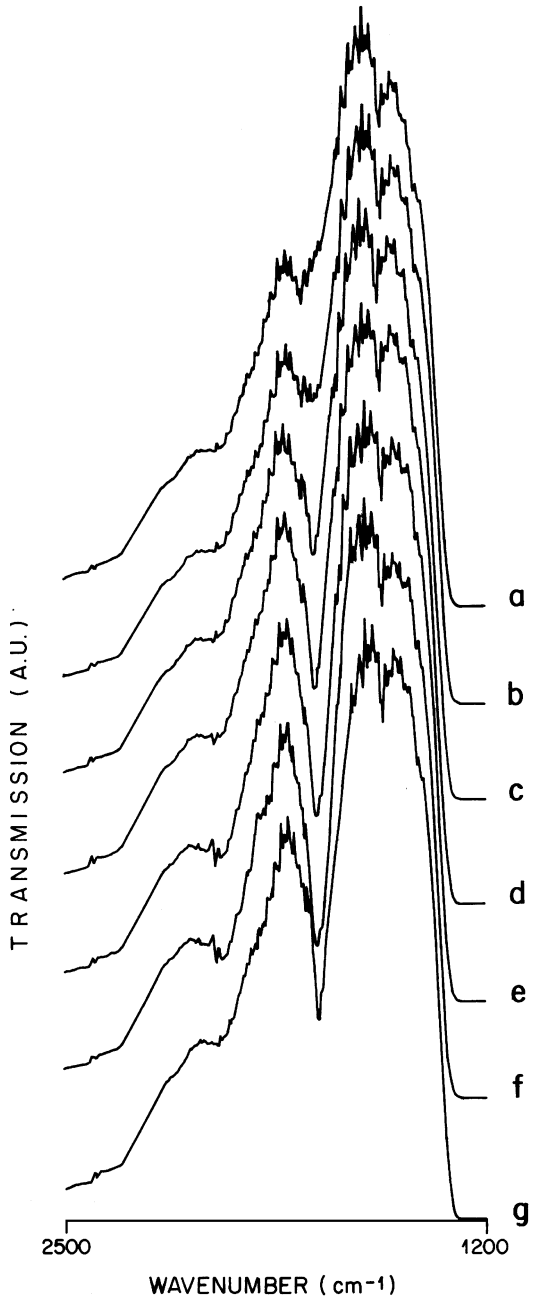

FIG. 5. Infrared spectra of nitric oxide adsorbed on the reduced CrAPSO-11 catalyst evacuated at 773 K (a) before adsorption of NO, (b) after adsorption of 2 Torr of NO, (c) after adsorption of 5 Torr of NO, (d) after adsorption of 15 Torr of NO, (e) after adsorption of 50 Torr of NO, (f) after adsorption of 50 Torr of NO for 90 min, and (g) after evacuation at room temperature for 60 min following procedure (f).

bands observed at ca. 1450 cm^{-1} and ca. 1547 cm^{-1} have been widely used in the literature (16, 18, 30) for assaying Lewis and Brønsted acidity on heterogeneous catalysts. The former corresponds to the 19b vibration of the Lewis bound pyridine. The band at ca. 1547 cm^{-1} has been assigned to pyridine adsorbed on Brønsted acid sites. Table 1 summarizes the number of Brønsted and Lewis sites (Brønsted and Lewis bound pyridine) for catalysts evacuated at 443, 623 and 723 K. It can be readily observed that the oxidic CrAPSO-11 catalyst has a higher acidity, Brønsted and Lewis (medium + strong acid sites), than both SAPO-11 catalysts and the supported system. For the reduced CrAPSO-11 catalyst, a large decrease for the strong acidity is observed (compared to the oxidic material), particularly for the Brønsted acidity. This decrease is not observed when the reduced Cr/SAPO-11 is compared to the supported oxidic sample.

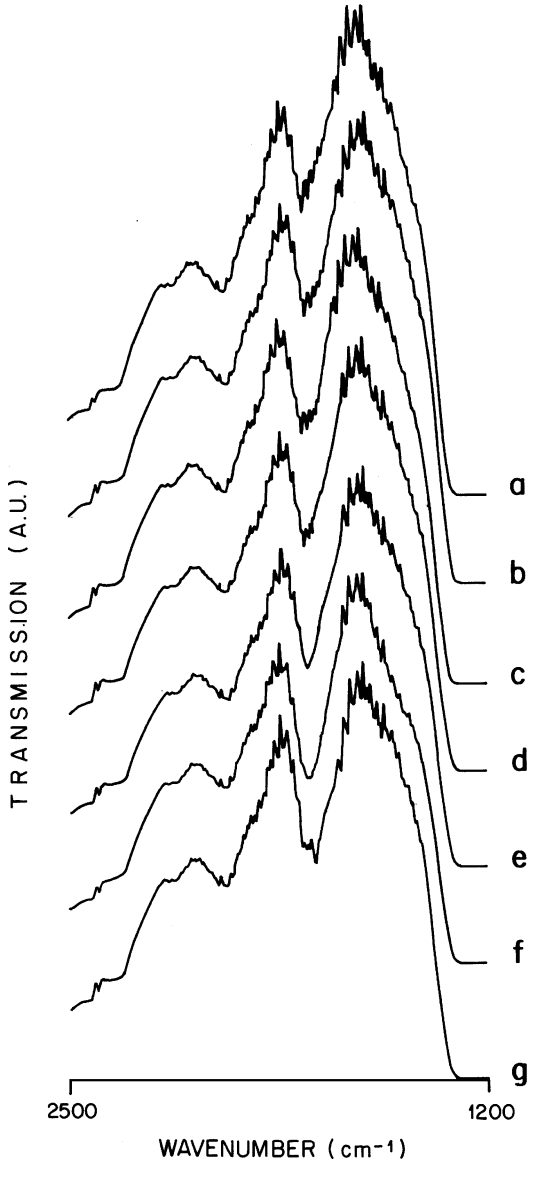

FIG. 6. Infrared spectra of nitric oxide adsorbed on the SAPO-11-A catalyst evacuated at 773 K (a) before adsorption of NO, (b) after adsorption of 2 Torr of NO, (c) after adsorption of 5 Torr of NO, (d) after adsorption of 15 Torr of NO, (e) after adsorption of 50 Torr of NO, (f) after adsorption of 50 Torr of NO for 90 min, and (g) after evacuation at room temperature for 60 min following procedure (f).

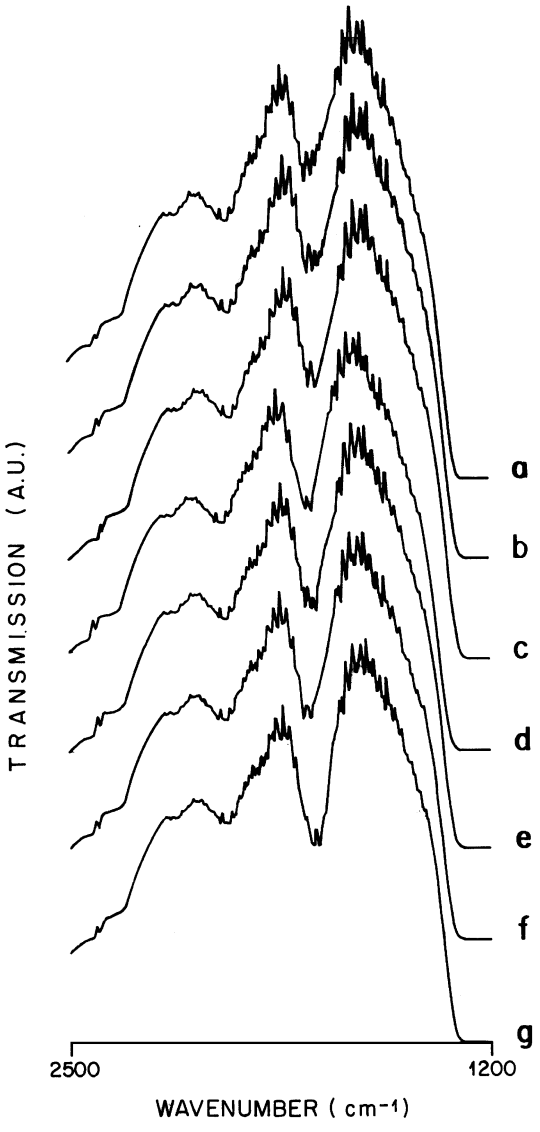

FIG. 7. Infrared spectra of nitric oxide adsorbed on the oxidic Cr/SAPO-11 catalyst evacuated at 773 K (a) before adsorption of NO, (b) after adsorption of 2 Torr of NO, (c) after adsorption of 5 Torr of NO, (d) after adsorption of 15 Torr of NO, (e) after adsorption of 50 Torr of NO, (f) after adsorption of 50 Torr of NO for 90 min, and (g) after evacuation at room temperature for 60 min following procedure (f).

For the sake of completion and due to the relevance of the previously published XPS and redox data (12) for the present work, it was decided to summarize the XPS results in Table 2. As observed, almost 70% of the chromium appears as Cr(VI) on the CrAPSO-11 catalyst, while only 18% of Cr(VI) was found on the supported solid. The reduction process (H_2, 773 K) decreases the Cr(VI) to 40% on the CrAPSO-11 catalyst and to 13% on the Cr/SAPO-11 solid. The redox cycles (H_2–O_2) strongly supported the XPS data (12).

The catalytic results are summarized in Tables 3–6. Both SAPO's showed greater stability than either chromium preparation. It is evident the decrease in the selectivity and in the SIE for the production of isobutene after 2.5 h, for the CrAPSO-11 catalyst. For lower TOS, the CrAPSO-11 catalyst showed the highest SIE, although the selectivity toward the formation of isobutene was very similar to that of SAPO-11-B and far superior to that shown by SAPO-11-A and the chromium supported system. The formation of C5+ hydrocarbons was also favored over the CrAPSO-11 and the SAPO-11-B solids. One of the most important catalytic results, however, is the much higher selectivity of the CrAPSO-11 system toward the formation of butadiene, particularly, when compared with the supported chromium system.

For the Cr/SAPO-11 catalyst, the selectivity towards isobutene is considerably smaller than for the CrAPSO-11 system, at low TOS. After 2.5 h it does not show, however, the abrupt decrease observed in the CrAPSO-11 catalyst. The cracking reactions and the production of C5+ hydrocarbons are considerably hindered over the supported system compared to the CrAPSO-11 sample.

The last column in Tables 3–6 is the specific activity for the skeletal isomerization reaction (SISA) (calculated on the basis of the number of medium + strong acid sites present

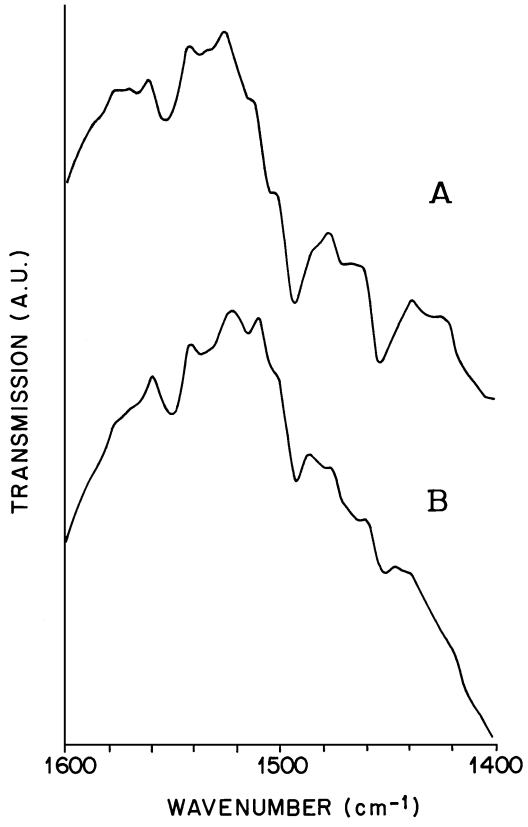

FIG. 8. Infrared spectra of pyridine adsorbed (A) on the oxidic CrAPSO-11 and (B) on the oxidic Cr/SAPO-11 catalysts after evacuation at 723 K.

TABLE 1

Amount of Brønsted (1547 cm^{-1}) and Lewis Bound Pyridine (1450 cm^{-1}) Calculated from IR Experiments[a]

Catalyst	Evacuation temperature (K)					
	443		623		723	
	1547 cm^{-1}	1450 cm^{-1}	1547 cm^{-1}	1450 cm^{-1}	1547 cm^{-1}	1450 cm^{-1}
SAPO-11-A	1.2	1.2	0.90	1.0	0.90	0.36
SAPO-11-B	2.0	1.7	2.0	1.3	2.0	1.2
Oxidic CrAPSO-11	3.2	2.2	2.7	2.2	2.0	1.4
Reduced CrAPSO-11	3.3	1.9	2.0	1.7	1.1	1.0
Oxidic Cr/APSO-11	5.0	2.5	1.8	1.7	1.3	0.59
Reduced Cr/SAPO-11	5.2	2.7	2.0	1.7	1.1	0.68

[a] The values are given in mmole of pyridine/g_{cat}.

on the oxidic catalysts). As observed the highest values correspond to the SAPO-11 systems, particularly for the SAPO-11-A, in apparent contradiction with the data shown previously. The SISA results, however, should be carefully examined, *vide infra*.

Finally, Table 7 shows a comparison between the number of medium + strong Brønsted acid sites, the Cr 2p (VI)/Al 2p intensity ratios (calculated from Table 2) and the SIE's for the different catalysts. As observed, the catalyst (CrAPSO-11) with the highest Cr(VI) 2p/Al 2p XPS intensity ratio is the one with the largest number of Brønsted acid sites and, at the same time, the catalyst that showed the largest SIE value.

DISCUSSION

The characterization and catalytic results obtained in this work show drastic differences between the CrAPSO-11 system and the supported Cr/SAPO-11 catalyst. The main differences found in the characterization work were the following:

1. DRS, XPS and redox cycles (12) data show an abundance of Cr(VI) for the oxidic CrAPSO-11 sample. A preponderance of Cr(III) was found for the oxidic supported material. The NO chemisorption experiments showed the presence of high chromium oxidation states on the oxidic CrAPSO-11. No evidence for the existence of the latter was observed for the supported oxidic system, thus, agreeing with the DRS and XPS results.

2. The distribution of oxidation states of chromium (XPS and NO chemisorption experiments) for the reduced CrAPSO-11 solid was different compared to the oxidic sample. Almost no differences were observed with the supported material.

3. The oxidic CrAPSO-11 catalyst showed an increase in the number of medium + strong acid sites compared to the other solids. The reduction process, however, decreased the Brønsted strong acid sites by a factor of two. A concomitant decrease in the number of medium + strong Lewis acid sites was also noted upon reduction. On the contrary, the supported sample showed a decrease in the number of medium and strong Brønsted acid sites compared to the CrAPSO-11 and SAPO-11-B solids. In this case, the reduction process did not cause major changes in the acidity distribution.

In our view, the majority of the data concerning the CrAPSO-11 catalyst support and reinforce the ideas presented by Chen and Sheldon (13a). These authors suggested a model which explained the increase in acidity observed for a calcined CrAPO-5 catalyst. The initial suggestion, confirmed by their data, was that for the assynthesized sample Cr(III) was octahedrally coordinated (with two extra water ligands) within the framework. Other studies by

TABLE 2

Percentage of Cr(VI) and Cr(III) and Cr 2p/Al 2p Intensity Ratios[a]

Catalyst	% Cr(VI)	% Cr(III)	Cr 2p/Al 2p
Oxidic CrAPSO-11	69	31	2.09
Reduced CrAPSO-11	40	60	2.06
Oxidic Cr/SAPO-11	18	82	2.07
Reduced Cr/SAPO-11	13	87	2.19

[a] Taken from Ref. 12. See text.

TABLE 3

Product Distribution for the Transformation of 1-Butene over SAPO-11-A[a]

Time on stream (h)	X	S_{iso}	$S_{2\text{-}b}$	S_{diene}	S_{C5+}	$S_{crack.}$	SIE	SISA
0.50	77.6	24.0	70.6	0	2.3	3.1	54.5	0.21
1.50	77.4	24.0	71.4	0.0	1.7	2.9	54.0	0.21
2.50	77.1	23.7	71.9	0.0	1.8	2.7	53.2	0.21
3.50	76.7	23.6	72.2	0.0	1.8	2.3	52.8	0.21
4.50	76.7	23.2	72.9	0.0	1.6	2.3	51.8	0.20
5.50	76.5	23.0	73.5	0.0	1.4	2.2	51.1	0.20
6.50	76.4	22.8	73.8	0.0	1.3	2.1	50.6	0.20

[a] For more details, see text.

TABLE 4

Product Distribution for the Transformation of 1-Butene over SAPO-11-B[a]

Time on stream (h)	X	S_{iso}	$S_{2\text{-}b}$	S_{diene}	S_{C5+}	$S_{crack.}$	SIE	SISA
0.50	82.8	36.7	53.5	0.1	5.5	4.0	87.3	0.15
1.50	82.4	36.5	54.9	0.1	5.9	3.4	85.7	0.15
2.50	82.1	36.2	56.3	0.1	4.9	3.0	84.0	0.15
3.50	82.2	35.5	56.6	0.6	4.6	2.9	82.7	0.15
4.50	81.8	35.9	57.4	0.6	3.5	2.7	82.6	0.15
5.50	81.8	35.4	57.9	0.6	3.7	2.9	81.4	0.15
6.50	81.7	35.1	57.9	0.6	4.3	2.6	81.0	0.15

[a] For more details, see text.

TABLE 6

Product Distribution for the Transformation of 1-Butene over Cr/SAPO-11[a]

Time on stream (h)	X	S_{iso}	$S_{2\text{-}b}$	S_{diene}	S_{C5+}	$S_{crack.}$	SIE	SISA
0.50	82.1	16.1	79.9	0.5	2.4	1.1	36.1	0.075
1.50	81.2	13.9	83.0	0.5	1.8	0.8	30.7	0.065
2.50	80.5	12.1	85.8	0.6	1.0	0.6	26.6	0.056
3.50	80.1	10.6	86.8	0.6	1.4	0.6	23.4	0.048
4.50	79.7	9.8	88.2	0.6	0.8	0.6	21.4	0.044
5.50	66.7	17.2	79.1	1.2	1.5	1.1	38.2	0.065
6.50	79.6	7.7	90.9	0.5	0.4	0.5	16.8	0.034

[a] For more details, see text.

Weckhuysen and Schoonheydt (20, 32) support the contention that in the as-synthesized CrAPO-5 molecular sieve, Cr(III) is octahedrally coordinated, irrespective of synthesis time, temperature, chromium source etc. Recently, we submitted results which showed the DRS spectra of Cr(III) for an as-synthesized CrAPO-11 sample (31). No Cr(VI) was observed. The preference of Cr(III) for octahedral coordination is well established and can be understood in terms of the Crystal Field Stabilization Energy (CFSE) of octahedral (224.5 KJ/mol) versus tetrahedral Cr(III) (66.9 KJ/mol) (20, 33). The second step in the model (13a), involved the formation, during the calcination process, of a dioxochromium (VI) species, still bonded to the internal aluminophosphate structure. In order to balance the charges, the formation of an acidic P–OH group was suggested. By using acetonitrile, the authors confirmed the presence of strong Lewis acid sites and acidic P–OH groups on the CrAPO-5 sample.

According to the mentioned model, if Cr(VI) is incorporated in the silicoaluminophosphate framework, it should be much more difficult to reduce than Cr(VI) supported on conventional supports, e.g., alumina, zirconia. Our XPS (Table 2) data shows a much higher stability of Cr(VI) towards reduction in the CrAPSO-11 sample compared to Cr/alumina catalysts (34, 35). The latter shows a higher extent of reduction at significantly lower temperatures (543 K). Moreover, the results for the NO chemisorption did not show appreciable amounts of Cr(III) dinitrosyl species for the reduced CrAPSO-11 sample. Under similar experimental conditions, this species has been reported as a major contributor of the IR spectra over reduced Cr/alumina (22), Cr/silica (36) and Cr/zirconia (24) catalysts.

The acidity measurements provide further support for the above model. The increase in Brønsted and Lewis acidity observed for the CrAPSO-11 sample, compared to the other solids, should be expected in terms of the ideas of Chen and Sheldon (13a). In addition, the decrease observed for the Lewis acidity during the reduction process, supports the contention that a coordinatively unsaturated Cr(VI) species bound to the molecular sieve framework, should exhibit the characteristics of strong Lewis acid sites (13a, 37, 38), as observed for CoAPOs (38). Concomitantly, the partial reduction of the Cr(VI) species is accompanied by a large decrease of the acidic P–OH groups, responsible of the Brønsted acidity (Table 7).

To further evaluate the feasibility of incorporation of Cr(VI) into the framework, successive ion exchange treatments of the calcined CrAPSO-11 sample with an

TABLE 5

Product Distribution for the Transformation of 1-Butene over CrAPSO-11[a]

Time on stream (h)	X	S_{iso}	$S_{2\text{-}b}$	S_{diene}	S_{C5+}	$S_{crack.}$	SIE	SISA
0.50	82.5	36.5	44.4	4.8	4.5	9.7	96.4	0.12
1.50	81.0	34.8	49.0	4.9	4.2	7.1	89.1	0.11
2.50	80.1	32.4	52.1	5.2	3.5	6.8	82.3	0.098
3.50	74.4	5.2	74.1	8.2	3.6	8.9	14.0	0.015
4.50	77.3	4.5	64.4	11.1	5.5	14.5	14.1	0.013
5.50	79.9	4.4	64.2	6.7	16.4	8.3	13.9	0.013
6.50	72.6	2.6	81.7	6.0	3.0	6.7	6.5	0.0072

[a] For more details, see text.

TABLE 7

Comparison of Acidity Measurements, XPS Data, and Catalytic Results

Catalyst	Ir[a] 1547 cm^{-1}	XPS Cr 2p(VI)/Al 2p[b]	SIE[c]
SAPO-11-A	0.90	—	54.5
SAPO-11-B	2.0	—	87.3
Oxidic CrAPSO-11	2.7	1.5	96.4
Reduced CrAPSO-11	2.0	0.8	—
Oxidic Cr/SAPO-11	1.8	0.4	36.1
Reduced Cr/SAPO-11	2.0	0.3	—

[a] Amount of medium + strong Brønsted acid sites, taken from Table 1.
[b] Calculated from Table 2.
[c] TOS = 0.5 h.

ammonium nitrate solution were performed. The results showed almost no loss of Cr(VI) from the calcined material. It is known from different studies (13a, 39, 40) that nonframework Cr(VI) species are easily extracted from calcined related materials by simply treating them with water. Thus, our results coincide with those of Chen and Sheldon (13a), strongly suggesting the incorporation of Cr(VI) into the molecular sieve framework.

Although, our data support the above conclusion, it should be noted, however that the incorporation of chromium into related molecular sieve frameworks is, by no means, a settled issue. Some authors have found for Cr-SAPO-34 (41) and CrAPO-5 (20, 32) catalysts, that Cr(III) is not incorporated into the molecular sieve framework during the synthesis procedure. Other studies (12, 13), have suggested the incorporation of tetrahedral Cr(VI), while another (42) has stressed the significant effect that the substitution of Al by Cr has on the framework. Different preparation and activation procedures, as well as the difficulty in the reproducibility of each critical step in the synthesis of these materials, may be responsible for the observed differences.

The catalytic results will now be analyzed in light of the above discussion. It has been reported (53, 54) that the acid strength required for acid-catalyzed transformations of hydrocarbons follows the following order: cracking $\sim$ oligomerization $>$ skeletal isomerization $\gg$ double bond isomerization. The increase in the medium + strong Brønsted and Lewis acidity observed for the oxidic CrAPSO-11 system, as a result of the highest amount of Cr(VI) (Table 7), is probably responsible for the higher selectivity towards isobutene, C5+ and cracking products found for this solid, for low TOS, when compared with the SAPO-11-A and with the supported system. Although, the CrAPSO-11 system shows a similar selectivity toward the formation of isobutene than the SAPO-11-B (at low TOS) and a similar S_{C5+}, its efficiency for the skeletal isomerization (SIE) is higher. This may arise from the following: double bond isomerization of 1-butene is much more facile, from an acidic viewpoint, than the skeletal isomerization (53, 54). As noted in Tables 4 and 5, at low TOS, particularly at TOS of 0.5 h, the selectivity towards 2-butenes is higher for the SAPO-11-B catalyst than for the CrAPSO-11 system, while the selectivity for the cracking and dehydrogenation reactions are higher for the CrAPSO-11 catalyst. If a fraction of the isomerized 2-butenes undergoes cracking and/or dehydrogenation, the net result would be a lower amount of 2-butenes (CrAPSO-11), rendering larger values for the Skeletal Isomerization Efficiency (SIE). Thus, the higher Brønsted acidity (Table 1), responsible for the cracking reactions and the higher dehydrogenation selectivity, found for the CrAPSO-11 system may account for the differences in SIE observed between the SAPO-11-B and the CrAPSO-11 catalysts, at low TOS.

After 2.5 h, for the CrAPSO-11 catalyst, the selectivity towards isobutene drops dramatically to less than 6% while the selectivity towards butadiene increases. These results can be, explained in terms of the reduction of Cr(VI) by the hydrocarbon stream, yielding a reduced catalyst with lower medium + strong Brønsted and Lewis acidity (Tables 1 and 7). The reduction of chromium catalysts by hydrocarbons is well established in the literature (43–45). It is generally accepted that high valence chromium is inactive for the dehydrogenation of hydrocarbons. Different studies suggest coordinatively unsaturated Cr(III) species as active sites for the dehydrogenation reaction (45–47), although earlier literature (48, 49) also considered the participation of Cr(II). In our case, the formation of Cr(III) species in the reduced CrAPSO-11 catalyst may explain the observed increase in butadiene. Interestingly enough, the observed "reduction process" is much more difficult than that observed for the dehydrogenation of *n*-butane over an unreduced 13% chromia/alumina catalyst (45). This can be understood in terms of differences in loading and the much higher stability towards reduction shown by the CrAPSO-11 (Table 2) compared with the conventional supported systems.

To further support the above discussion, the following experiment was performed: An oxidic sample of CrAPSO-11 catalyst was pre-reduced for 3 h with pure H_2 at 773 K, followed by the catalytic reaction under identical experimental conditions. The main result was that for a TOS of 0.5 h, the selectivity towards isobutene was 5.5, which is basically the same value obtained after 3.5 h, for the reaction performed on the oxidic material. This result strongly supports the above discussion., viz, as chromium is reduced the selectivity towards the formation of isobutene decreases (Table 7).

In all fairness, however, it should be noted that the huge decrease in isobutene formation, for high TOS, is not accompanied by a decrease in the formation of C5+ hydrocarbons and cracking reactions. This result seems to suggest that factors other than the decrease and/or deactivation of medium + strong acid sites may be responsible for the selective decrease in the formation of isobutene. It has been shown that topological parameters, associated with the intracrystalline spaciousness, may play an important role on the selectivity towards isobutene, during the transformations of *n*-butenes (6). How the reduction process could affect these topological parameters, is an issue that has to be further investigated.

A comment concerning the specific activities for the skeletal isomerization (SISA) is in order. As shown in Tables 3–6 the higher values are obtained over the two SAPO-11 systems. Worthy of mention is the fact that if the SISA values are normalized per crystalline fraction (14), an almost identical value is obtained for both SAPO-11 samples. This observation is in agreement with the expected behavior of AEL structures, having a similar

framework-silicon content, incorporated through the same substitution mechanism (14).

There is a problem, however, when these specific activities are compared, particularly, with the CrAPSO-11 catalyst. The latter undergoes reduction during the catalytic reactions, with a concomitant decrease in the number of medium and strong Brønsted acid sites. The calculated SISA is based on the acid sites present on the oxidic material. In order to estimate the "real SISA values" for the CrAPSO-11 system, the actual number of Brønsted medium + strong acid sites, under reaction conditions, would have to be considered. Unfortunately, these data are unknown. Therefore, the SISA values have to be examined very carefully before reaching any conclusions. Furthermore, the very low values for SISA observed for the CrAPSO-11 catalyst (Table 5), at high TOS (>3.5 h), may reflect, not only the uncertainty in the actual number of sites, but also a decrease in acid strength (change in the nature of the acid site).

On the other hand, the supported Cr/SAPO-11 catalyst does not show the sharp decrease in the production of isobutene while showing a much lower SIE (36.1% at best) for low times-on-stream. These results agree with the fact that over this oxidic catalyst the Brønsted and Lewis acidity are considerably lower and that the distribution of oxidation states for chromium is barely modified by the reduction process (Table 2). According to the above discussion, a small difference in the medium + strong Brønsted and Lewis acidity is expected as a result of the reduction process. Table 1 confirms the latter.

Interestingly enough, the production of butadiene for the supported catalyst is almost ten times lower than for the CrAPSO-11 system. It is known that both (the oxidic and reduced) versions of Cr/SAPO-11, consist of mainly Cr(III). Why, then, the low production of butadiene? Table 2 indicates that for the supported catalyst, Cr(III) shows an unexpected stability during oxidation at 773 K. It is possible that chromia species were formed during the calcination process over this catalyst. These species are known to be exceedingly difficult to oxidize under our experimental conditions (13b, 50). Moreover, the similar Cr 2p/Al 2p intensity ratios (Table 2) obtained for both oxidic preparations, despite the higher chromium content of the supported system, strongly suggests larger particle sizes on the Cr/SAPO-11 catalyst. Thus, agreeing with the formation of chromia. Seemingly, these chromia species have a low degree of coordinative unsaturation, since there was no observable NO chemisorption by IR on this catalyst. Probably, these high clustered, poorly exposed, chromia species are responsible for the low production of butadiene over this catalyst. Another possibility, for the low production of butadiene, is the formation of highly stabilized Cr(III) ions by the support. Reports in the literature (45, 50) indicate that only the Cr(III) species arising from higher valence states are coordinatively unsaturated and, thus, active for the dehydrogenation reaction.

Finally, the possibility of existence of Cr(V) has to be addressed. This species has repeatedly been reported in some studies dealing with chromium catalysts (13b, 24, 47, 52). In our work, large amounts of Cr(V) are not likely due to the following: a) excellent correlation between the curve fitting results (12), where only Cr(VI) and Cr(III) were considered, and the redox data (H_2–O_2) cycles. Preliminary ESR results (52) have shown the presence of no more than 8% of Cr(V) for both catalysts. Minor amounts of Cr(V), however, can not be ruled out.

CONCLUSIONS

1. A large fraction of Cr(VI) was found by DRS and XPS, for the oxidic CrAPSO-11 sample. XPS showed almost 70% of the chromium existed as Cr(VI). A preponderance of Cr(III) was found for the oxidic supported material (~82%). The NO chemisorption experiments showed the presence of high chromium oxidation states on the oxidic CrAPSO-11, thus, agreeing with the DRS and XPS results. No evidence for the existence of the mentioned states was observed for the supported oxidic system.

2. The distribution of oxidation states of chromium (XPS and NO chemisorption experiments) for the reduced CrAPSO-11 solid, was different (~40% Cr(VI) and ~60% Cr(III)) compared to the oxidic sample. Almost no differences were observed with the Cr/SAPO-11 catalyst.

3. The oxidic CrAPSO-11 catalyst showed the highest number of medium + strong acid sites compared to the other solids. The reduction process, however, decreased the Brønsted strong acid sites by a factor of two. A concomitant decrease was observed for the medium and strong Lewis acid sites upon reduction. These results suggest that a partially unsaturated Cr(VI) in the vecinity of P–OH groups may act as strong Lewis sites, generating Brønsted acidity by Brønsted-Lewis interaction (as suggested by Chen and Sheldon). On the contrary, the supported sample showed a reduction of medium + strong acid sites compared to the CrAPSO-11 and SAPO-11-B catalysts. In this case, the reduction process did not cause major changes in the acidity distribution.

4. The CrAPSO-11 catalyst showed a higher efficiency (SIE) towards the formation of isobutene, for times-on-stream < 2.5 h, than the SAPO-11 catalysts and the supported chromium system. The skeletal isomerization selectivity was, however, similar to that of SAPO-11-B. After 2.5 h a drastic decrease in the selectivity occurred with a concomitant increase in the formation of butadiene and 2-butenes. Changes in acidity, that occured during the reduction process of the Cr(VI) species by the hydrocarbon stream, may explain the differences in the selectivity towards isobutene. No such effects were observed for the

supported system. The CrAPSO-11 catalyst was, by far, the best dehydrogenation catalyst.

The characterization as well as the catalytic data support and reinforce the model presented by Chen and Sheldon (13a) for CrAPO-5. The results suggest the incorporation of chromium into the molecular sieve framework for the CrAPSO-11 catalyst.

ACKNOWLEDGMENT

This work was supported by Consejo Nacional de Investigaciones Científicas y Tecnológicas (CONICIT) through Grant-RPI-10001.

REFERENCES

1. Pines, H., "The Chemistry of Catalytic Hydrocarbon Conversions." Academic Press, New York, 1981.
2. Brouwer, D. M., and Oelderik, J. M., *Rec. Trav. Chim. Pays-bas* **87**, 721 (1968).
3. Brouwer, D. M., and Hogeveen, H., *Progr, Phys. Org. Chem.* **9**, 179 (1972).
4. Choudhary, V. R., *Chem. Ind. Dev.* **8**(7), 32 (1974).
5. (a) Cheng, Z. X., and Ponec, V., *J. Catal.* **148**, 607 (1995); (b) Guisnet, M., Andy, P., Gnep, G., Benazzi, E., and Travers, C., *J. Catal.* **158**, 551 (1996).
6. Mooiweer, H. H., de Jong, K. P., Kraushaar-Czarnetzki, B., Stork, W. H. J., and Krutzen, B. C. H., *in* "Zeolites and Related Microporous Materials: State of the Art 1994" (J. Weitkamp, H. G. Karge, H. Pfeifer, and W. Hölderich, Eds.), Studies in Surface Science and Catalysis, Vol 84, p. 2327. Elsevier, Amsterdam, 1994.
7. Simon, M. W., Suib, S. L., and O'Young, Chi-Lin., *J. Catal.* **147**, 484 (1994).
8. Maxwell, I. E., and Naber, J. E., *Catal. Lett.* **12**, 105 (1992).
9. (a) Zubowa, H.-L., Richter, M., Roost, U., Parlitz, B., and Fricke, R., *Catal. Lett.* **19**, 67 (1993); (b) Gajda, G. J., U.S. patent 5132484 (1991).
10. Escalante, D., López, C. M., Machado, F. J., Matjushing, M., Méndez, B., Pinto, M., and Ramírez-Agudelo, M. M., *in* "Environmental Catalysis" (G. Centi, C. Cristiani, P. Forzatti, and S. Perathoner, Eds.), p. 415. SCI Pub., Rome, 1995.
11. Escalante, D., Goldwasser, J., López, C. M., Machado, F. J., Pinto, M., and Ramírez-Agudelo, M. M., *in* "Proceedings of the XV Iberoamerican Symposium on Catalysis" (E. Herrero, O. Anunziata, and C. Pérez, Eds.), Vol. 1, p. 103, Córdoba, Argentina, 1996.
12. Giraldo, L., Pfaff, C., López, C. M., Machado, F., Méndez, B., Goldwasser, J., Ramírez de Agudelo, M. M., Rondón, S., Houalla, M., and Hercules, D. M., *Surf. Interface Anal.* **24**, 863 (1996).
13. (a) Chen, J. D., and Sheldon, R. A., *J. Catal.* **153**, 1 (1995); (b) Poole, C. P., Jr., and MacIver, D. S., *Adv. Catal.* **17**, 223 (1967).
14. Alfonzo, M., Goldwasser, J., López, C. M., Machado, F. J., Matjushin, M., Méndez, B., and Ramírez de Agudelo, M. M., *J. Mol. Catal.* **98**, 35 (1995).
15. Goldwasser, J., Houalla, M., Fang, S. M., and Hall, W. K., *J. Catal.* **115**, 34 (1989).
16. Pantoja, A., Sarrín, J., González, L., Noguera, O., Pérez Zurita, M. J., Galavís, J. L., and Goldwasser, J., *J. Catal.* **142**, 110 (1993).
17. (a) Goldwasser, M. R., Rojas, D., and Goldwasser, J., *J. Catal.* **135**, 596 (1992); (b) Emeis, C. A., *J. Catal.* **141**, 347 (1993).
18. Segawa, K. I., and Hall, W. K., *J. Catal.* **76**, 133 (1982).
19. Flanigen, E. M., Lok, B. M. T., Patton, R. L., and Wilson, S. T., U.S. patent 4738837 (1988).
20. Weckhuysen, B. M., and Schoonheydt, R. A., *Zeolites* **14**, 360 (1994).
21. Lever, A. B. P., "Inorganic Electronic Spectroscopy," 2nd ed. Elsevier, Amsterdam, 1984.
22. Peri, J. B., *J. Phys. Chem.* **78**, 588 (1974).
23. Zecchina, A., Garrone, E., Morterra, C., and Coluccia, S., *J. Phys. Chem.* **79**, 978 (1975).
24. Ghiotti, G., and Chiorino, A., *Spectrochimica Acta* **49A** (9), 1345 (1993).
25. Ward, J. W., *in* "Zeolite Chemistry and Catalysis" (J. A. Rabo, Ed.), ACS monograph 171, p. 202. Washington, 1976.
26. Nakamoto, K., "Infrared Spectra of Inorganic and Coordination Compounds." Wiley, New York, 1963.
27. Arakawa, E. T., and Nielsen, A. H., *J. Mol. Spectroscopy* **2**, 413 (1958).
28. Begun, G. M., *J. Mol. Spectroscopy* **4**, 388 (1960).
29. Snyder, R. G., and Hisatsune, I. C., *J. Mol. Spectroscopy* **1**, 139 (1957).
30. Kiviat, F. E., and Petrakis, L., *J. Phys. Chem.* **77**, 1232 (1973).
31. Arias, D., Campos, I., Escalante, D., Goldwasser, J., López, C. M., Machado, F., Méndez, B., Moronta, D., Pinto, M., Ramírez de Agudelo, M. M., and Sazo, V., *J. Mol. Catal.*, in press.
32. Weckhuysen, B. M., and Schoonheydt, R. A., *in* "Zeolites and Related Microporous Materials: State of the Art 1994" (J. Weitkamp, H. G. Karge, H. Pfeifer, and W. Hölderich, Eds.)., Studies in Surface Science and Catalysis, Vol. 84, p. 965. Elsevier, Amsterdam, 1994.
33. West, A. R., "Basic Solid State Chemistry," Wiley, Chichester, 1988.
34. Scierka, S. J., Proctor, A., Houalla, M., Fiedor, J. N., and Hercules, D. M., *Surf. Interface Anal.* **20**, 901 (1993).
35. Scierka, S. J., Houalla, M., Proctor, A., and Hercules, D. M., *J. Phys. Chem.* **99**, 1537 (1995). [See references therein]
36. Kugler, E. L., Kokes, R. J., and Gryder, J. W., *J. Catal.* **36**, 142 (1975).
37. Cornaro, U., Jiru, P., Tvaruzkova, Z., and Habersberger, K., *in* "Zeolite Chemistry and Catalysis" (P. A. Jacobs, N. I. Jaeger, and L. Kubelkova, Eds.), p. 165. Elsevier, Amsterdam, 1991.
38. Jänchen, J., Peeters, M. P. J., van Wolput, J. H. M. C., Wolthuizen, J. P., van Hooff, J. H. C., and Lohse, U., *J. Chem. Soc. Faraday Trans.* **90**, 1033 (1994).
39. Mambrin, J. S. T., Vichi, E. J. S., Pastore, H. O., Davanzo, C. U., Vargas, H., Silva, E., and Nakamura, O., *J. Chem. Soc., Chem. Commun.* 922 (1991).
40. Hemidy, J. F., and Cornet, D., *J. Chim. Phys.* **5**, 739 (1974).
41. Rajic, N., Stojakovic, D., Hocevar, S., and Kaulik, V., *Zeolites* **14**, 360 (1993).
42. Peeters, M. P. J., van de Ven, L. J. M., de Haan, J. W., and van Hooff, J. H. C., *Colloids Surf.* **A 72**, 87 (1993).
43. Grünert, W., Saffert, W., Feldhaus, R., and Anders, K., *J. Catal.* **100**, 138 (1986).
44. Gorriz, O. F., Cortés Corbéran, V., and Fierro, J. L. G., *Ind. Eng. Chem. Res.* **31**, 2670 (1992).
45. Hakuli, A., Kytökivi, A., Krause, O. I., and Suntola, T., *J. Catal.* **161**, 393 (1996).
46. Masson, J., Bonnier, J. M., Duvigneaud, P. H., and Delmon, B., *J. Chem. Soc. Faraday Trans.* **173**, 1471 (1977).
47. De Rossi, S., Ferraris, G., Fremiotti, S., Garrone, E., Ghiotti, G., Campa, M. C., and Indovina, V., *J. Catal.* **148**, 36 (1994).
48. Ashmawy, F. M., *J. Chem. Soc. Faraday Trans.* **176**, 2096 (1980).
49. Lugo, H. J., and Lunsford, J. H., *J. Catal.* **91**, 155 (1985).
50. MacDaniel, *Adv. Catal.* **33**, 47 (1985).
51. De Rossi, S., Ferraris, G., Fremiotti, S., Indovina, V., and Cimino, A., *Appl. Catal.* **106**, 125 (1993).
52. Machado, F., López, C. M., Moronta, D., Ramírez de Agudelo, M. M., and Goldwasser, J., unpublished results.
53. Corma, A., and Wojciechowski, B., *Catal. Rev. Sci. Eng.* **24**, 1 (1982).
54. O'Young, Chi-Lin., Wen-Qing, Xu, Simon, M., and Suib, S. L., *in* "Zeolites and Related Microporous Materials: State of the Art 1994" (J. Weitkamp, H. G. Karge, H. Pfeifer, and W. Hölderich, Eds.), Studies in Surface Science and Catalysis, Vol. 84, p. 1671. Elsevier, Amsterdam, 1994.